Supporting information:

Ultralong $CH_3NH_3PbI_3$ nanowires synthesized by ligand-assisted reprecipitation strategy for high-performance photodetector

*Xu He [a,b], Chuanyong Jian [a, c], Wenting Hong [a, c], Qian Cai [a,b], and Wei Liu [*a, b]*

[a]*Key Laboratory of Design and Assembly of Functional Nanostructures, and Fujian Provincial Key Laboratory of Nanomaterials, Fujian Institute of Research on the Structure of Matter, Chinese Academy of Sciences, Fuzhou, Fujian, 350002, P. R. China.*

[b]*Fujian Science & Technology Innovation Laboratory for Optoelectronic Information of China, Fuzhou, Fujian 350108, P. R. China*

[c]*University of Chinese Academy of Sciences, Beijing, 100049, China.*

E-mail: liuw@fjirsm.ac.cn

Preparation of $CH_3NH_3PbI_3$ nanowires

The precursor solution is prepared by dissolving 1 mmol CH_3NH_3I and PbI_2 into 1 ml dimethylformamide (DMF) solvent, followed by stirring at 70 °C water for 6 hours. The different volume of oleylamine varying from 0 to 30 μl is dropped into 50 μl of the prepared precursor solution. Then, 1 ml toluene is injected into the obtained precursor solution. After ultrasonic shaking, the mixed solution is centrifuged at 3000 rpm for 5 minutes. The supernatant is removed, and the obtained nanowires precipitate washed by toluene several times.

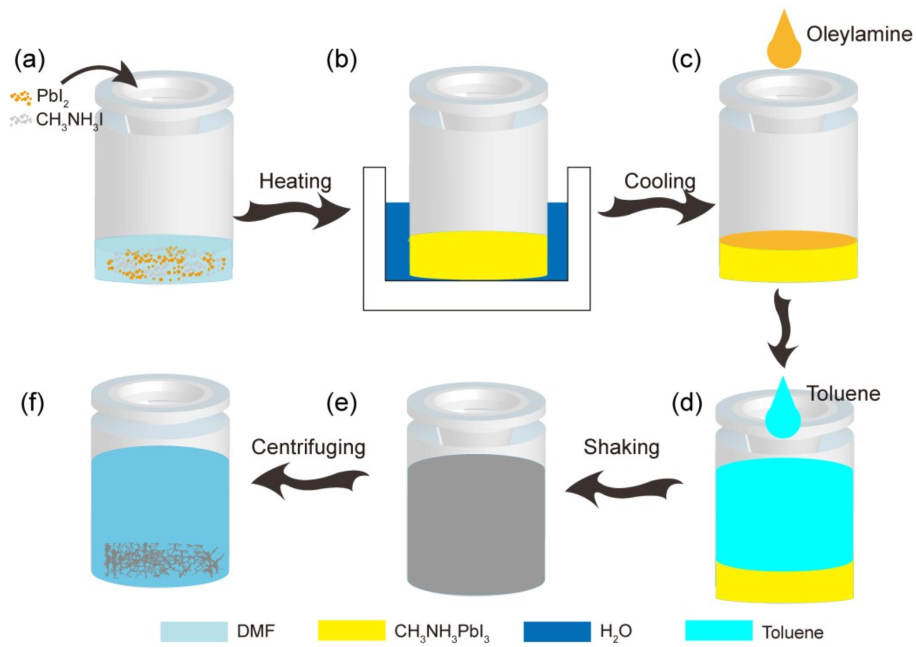

Fig. S1. Schematic illustration of the modified LARP strategy for the fabrication of $CH_3NH_3PbI_3$ nanowires.

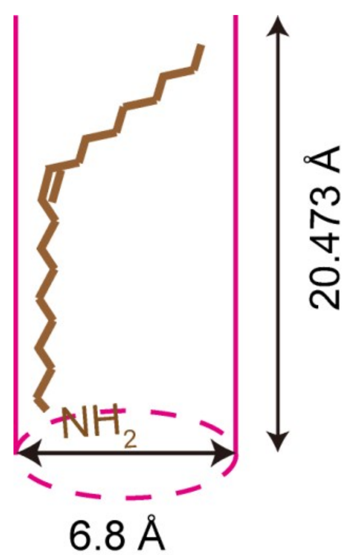

Fig. S2. The chemical structure of oleylamine.

Table S1. Comparison of the preparation methods, length, crystal qualities and morphologies of the perovskite nanowires in this work and these in literature.

Materials	**Methods**	**Length**	**Surface defects**	**Morphologies**	**Ref.**
$CH_3NH_3PbI_3$	Modified LARP	Several millimeters	Low	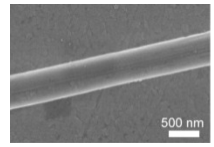	Our work
$CH_3NH_3PbI_3$	Evaporation-induced self-assembly process	300 μm	Low	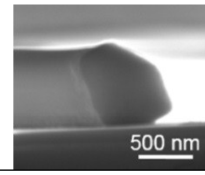	1
$CsPbBr_3$	One-step CVD	Several millimeters	Low	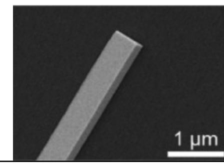	2
$CH_3NH_3PbI_3$	Slip-coating process	16 μm	High	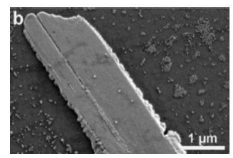	3
$CH_3NH_3PbI_3$	Template-assisted	Several millimeters	High	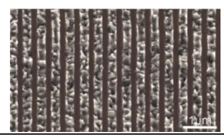	4
$CH_3NH_3PbI_3$	Two-step CVD	20 μm	Low	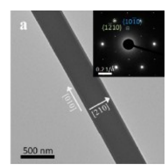	5
$CH_3NH_3PbI_3$	Two-step solution-phase	~20 μm	Low	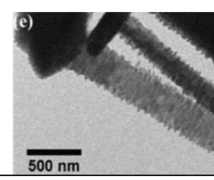	6

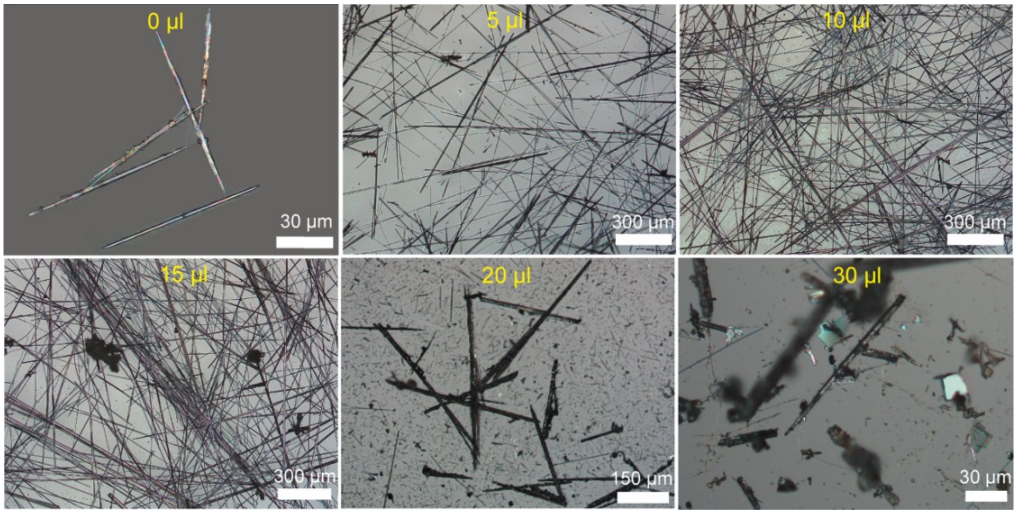

Fig. S3. The optical microscope of the as-prepared $CH_3NH_3PbI_3$ nanowires obtained by the LARP strategy with the addition of oleylamine changed from 0 μl to 30 μl.

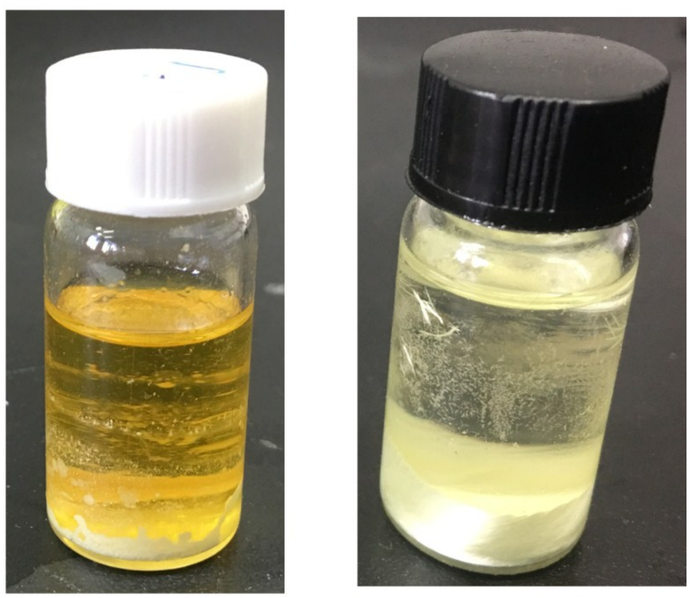

Traditional LARP strategy Modified LARP strategy

Fig. S4. The photographs of the product yields of nanowires prepared by the traditional LARP strategy and our modified LARP strategy (the addition of oleylamine is 10 μl).

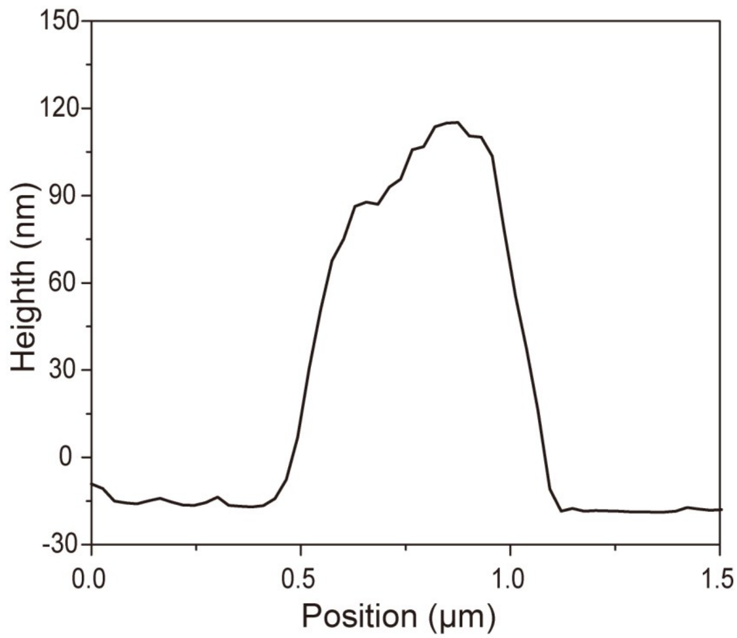

Fig. S5. The height distribution of the area of single Om-$CH_3NH_3PbI_3$ nanowire marked by the red wire in Fig. 3g.

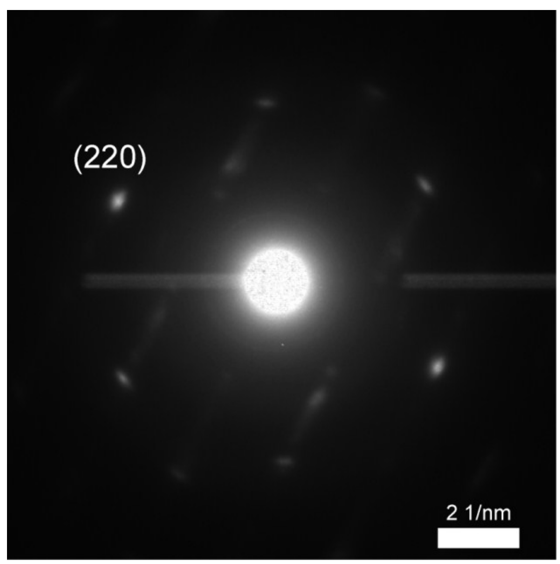

Fig. S6. The corresponding selected-area diffraction (SAED) pattern of Om-$CH_3NH_3PbI_3$ nanowire.

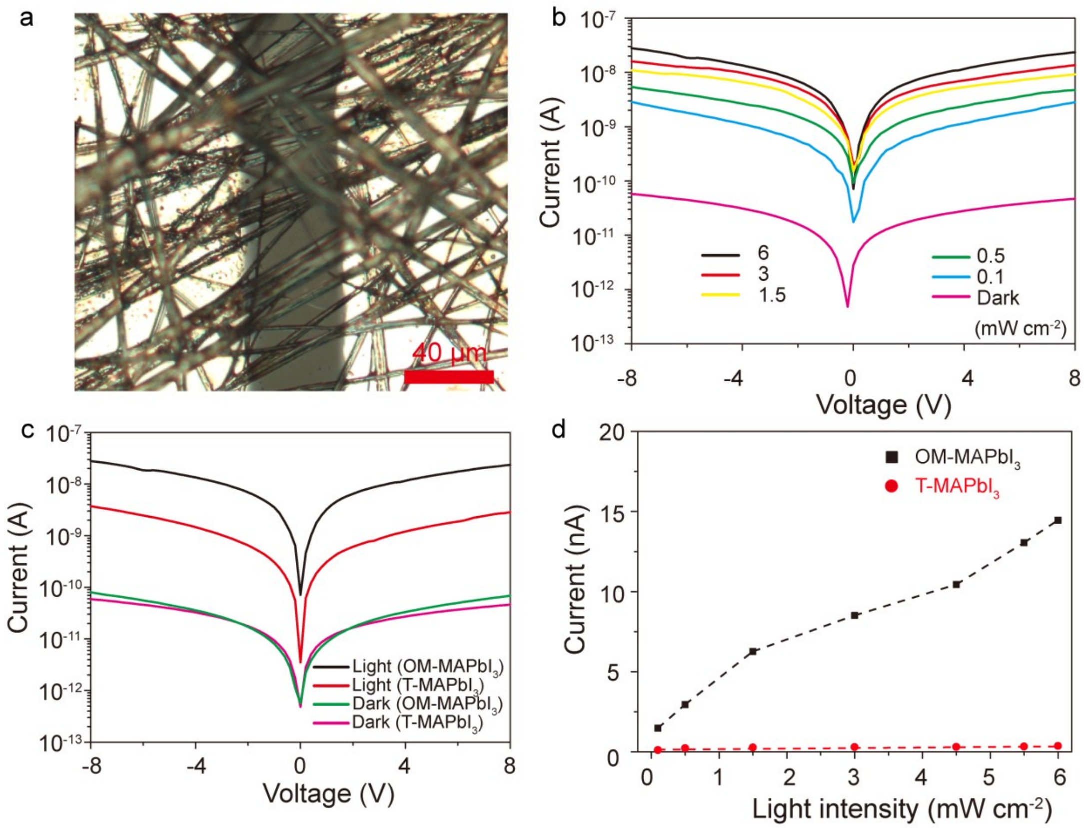

Fig. S7. (a) Schematic device structure diagram and optic microscope image for high-density Om-$CH_3NH_3PbI_3$ nanowires photodetector. (b) The high-density Om-$CH_3NH_3PbI_3$ nanowires photodetector under different power intensity ranging from 0 to 6 mW cm^{-2}. (c) I-V curves of the high-density Om-$CH_3NH_3PbI_3$ and T-$CH_3NH_3PbI_3$ nanowires photodetector in the dark and under the light. The light intensity was 6 mW cm^{-2}. (d) The dependence of photocurrent on power intensity at a bias of +5 V.

As shown in Figure S3a, high-density Om-$CH_3NH_3PbI_3$ nanowires are spinning coating onto the pretreated substrate, and 100 nm Al electrode are then thermally evaporated through shadow masks with a channel length of 0.5 mm and channel width of 40 μm to form photodetectors. Figure S3b shows the I-V curves of the devices measured in the dark and under white light illumination with light power intensity ranging from 0.1 to 6 mW cm^{-2}. For the Om-$CH_3NH_3PbI_3$

nanowires, the device current is very low (about 3.3×10^{-11} A at 5 V) in the dark, whereas the photocurrent increases remarkably by about 100 times under 0.1 mW cm^{-2} light illumination. For comparison, the device based on T-$CH_3NH_3PbI_3$ nanowires is also detected and the results are compared to that of Om-$CH_3NH_3PbI_3$ nanowires device as shown in Figure S3c. As expected, the Om-$CH_3NH_3PbI_3$ nanowires device shows about 10 times current higher than the T-$CH_3NH_3PbI_3$ nanowires device under the white light illumination. Furthermore, as shown in Figure S3d, the devices are characterized by plotting the light intensity-dependent photocurrent curves under white light illumination at +5 V bias. The slope for Om-$CH_3NH_3PbI_3$ nanowire photodetector is higher than that of T-$CH_3NH_3PbI_3$ nanowire photodetector, reveals the reduction of the recombination centers in Om-$CH_3NH_3PbI_3$ nanowire as compared to T-$CH_3NH_3PbI_3$ nanowire.

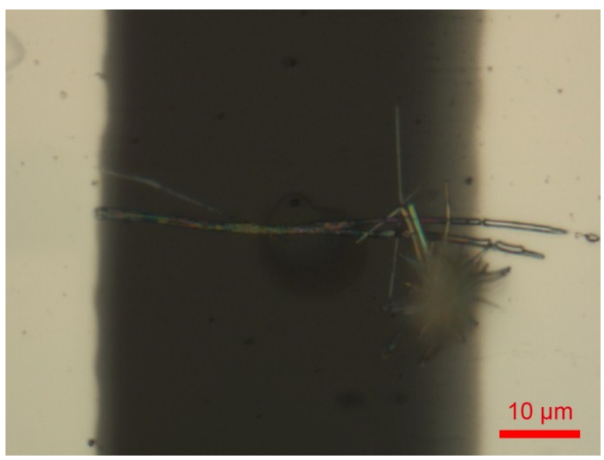

Fig. S8. Optic microscope image for single T-$CH_3NH_3PbI_3$ nanowire photodetector.

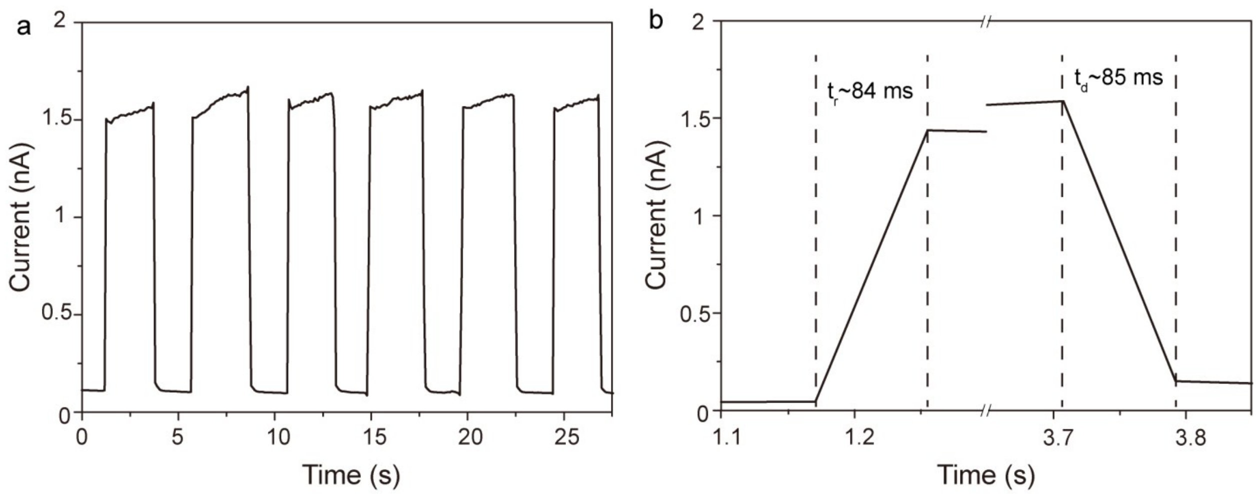

Fig. S9. (a) Time-dependent photoresponse of the device under the power intensity of 6 mW cm^{-2} at a bias of 8V. (b) Photocurrent rise and decay of the device measured at a bias of 8V and a light intensity of 6 mW cm^{-2}.

Table S2. Performance comparison of our $CH_3NH_3PbI_3$ nanowire-based photodetector with other $CH_3NH_3PbI_3$ nanowire-based devices in the literature.

Materials	**Responsivity (A/W)**	**Detectivity (×10^{12} Jones)**	**Ref.**
$CH_3NH_3PbI_3$ nanowire	11.36	1.48	Our work
$CH_3NH_3PbI_3$ network	0.1	1.02	7
$CH_3NH_3PbI_3$	~36	~0.01	8
$CH_3NH_3PbI_3$ nanowire	4.95	20 (M)	9
$CH_3NH_3PbI_3$ microwire	13.85	3.87	10
$CH_3NH_3PbI_3$ microwire	1.2	2.39	11
$CH_3NH_3PbI_3$ microwire	0.48	1.26	12
$CH_3NH_3PbI_3$ nanowire	1.3	2.5	13

Note: (M) represents for measured noise

Referecnes

[1] X. Xu, X. Zhang, W. Deng, L. Huang, W. Wang, J. Jie, X. Zhang. Saturated Vapor-Assisted Growth of Single-Crystalline Organic-Inorganic Hybrid Perovskite Nanowires for High-Performance Photodetectors with Robust Stability. ACS Appl. Mater. Interfaces 10 (2018) 10287-10295.

[2] M. Shoaib, X. Zhang, X. Wang, H. Zhou, T. Xu, X. Wang, X. Hu, H. Liu, X. Fan, W. Zheng, T. Yang, S. Yang, Q. Zhang, X. Zhu, L. Sun, A. Pan. Directional Growth of Ultralong $CsPbBr_3$ Perovskite Nanowires for High-Performance Photodetectors. J. Am. Chem. Soc. 139 (2017) 15592-15595.

[3] E. Horvath, M. Spina, Z. Szekrenyes, K. Kamaras, R. Gaal, D. Gachet, L. Forro. Nanowires of methylammonium lead iodide ($CH_3NH_3PbI_3$) prepared by low temperature solution-mediated crystallization. Nano Lett 14 (2014) 6761-6766.

[4] M. Spina, E. Bonvin, A. Sienkiewicz, B. Nafradi, L. Forro, E. Horvath. Controlled growth of $CH_3NH_3PbI_3$ nanowires in arrays of open nanofluidic channels. Sci. Rep. 6 (2016) 19834.

[5] J. Xing, X.F. Liu, Q. Zhang, S.T. Ha, Y.W. Yuan, C. Shen, T.C. Sum, Q. Xiong. Vapor Phase Synthesis of Organometal Halide Perovskite Nanowires for Tunable Room-Temperature Nanolasers. Nano Lett 15 (2015) 4571-4577.

[6] P.V. Chandrasekar, S. Yang, J. Hu, M. Sulaman, Y. Shi, M.I. Saleem, Y. Tang, Y. Jiang, B. Zou. Solution-phase, template-free synthesis of PbI_2 and $MAPbI_3$ nano/microtubes for high-sensitivity photodetectors. Nanoscale 11 (2019) 5188-5196.

[7] H. Deng, X. Yang, D. Dong, B. Li, D. Yang, S. Yuan, K. Qiao, Y.B. Cheng, J. Tang, H. Song. Flexible and Semitransparent Organolead Triiodide Perovskite Network Photodetector Arrays with High Stability. Nano Lett 15 (2015) 7963-7969.

[8] L. Gu, M.M. Tavakoli, D. Zhang, Q. Zhang, A. Waleed, Y. Xiao, K.H. Tsui, Y. Lin, L. Liao,

J. Wang, Z. Fan. 3D Arrays of 1024-Pixel Image Sensors based on Lead Halide Perovskite Nanowires. Adv. Mater. 28 (2016) 9713-9721.

[9] L. Gao, K. Zeng, J. Guo, C. Ge, J. Du, Y. Zhao, C. Chen, H. Deng, Y. He, H. Song, G. Niu, J. Tang. Passivated Single-Crystalline CH3NH3PbI3 Nanowire Photodetector with High Detectivity and Polarization Sensitivity. Nano Lett 16 (2016) 7446-7454.

[10] Y. Chen, J. Zhang, J. Zhou, Y. Chu, B. Zhou, X. Wu, J. Huang. Long-Term Stable and Tunable High-Performance Photodetectors Based on Perovskite Microwires. Adv. Opt. Mater. 6 (2018) 1800469.

[11] Y. Liu, F. Li, C. Perumal Veeramalai, W. Chen, T. Guo, C. Wu, T.W. Kim. Inkjet-Printed Photodetector Arrays Based on Hybrid Perovskite CH3NH3PbI3 Microwires. ACS Appl. Mater. Interfaces 9 (2017) 11662-11668.

[12] J. Li, Y. Liu, X. Ren, Z. Yang, R. Li, H. Su, X. Yang, J. Xu, H. Xu, J.-Y. Hu, A. Amassian, K. Zhao, S.F. Liu. Solution Coating of Superior Large-Area Flexible Perovskite Thin Films with Controlled Crystal Packing. Adv. Opt. Mater. 5 (2017) 1700102.

[13] H. Deng, D. Dong, K. Qiao, L. Bu, B. Li, D. Yang, H.E. Wang, Y. Cheng, Z. Zhao, J. Tang, H. Song. Growth, patterning and alignment of organolead iodide perovskite nanowires for optoelectronic devices. Nanoscale 7 (2015) 4163-4170.